Journal of the European Ceramic Society 23 (2003) 357–369
www.elsevier.com/locate/jeurceramsoc

# Oxidation resistance of AlN–($TiB_2$–$TiSi_2$) ceramics in air up to 1450 °C

V.A. Lavrenko[a,*], J. Desmaison[b], A.D. Panasyuk[a], M. Desmaison-Brut[b]

[a]*Institute for Problems of Materials Science, 3 Krzhyzhanovsky str., 03680 Kiev-142, Ukraine*
[b]*Laboratoire de Science des Procedes Ceramiques et de Traitements de Surface, SPCTS UMR CNRS 6638, 123, Avenue Albert Thomas, 87060 Limoges Cedex, France*

Received 5 December 2001; received in revised form 12 May 2002; accepted 25 May 2002

**Abstract**

With the aid of DTA, TG, XRD, SEM and EPMA methods the kinetics and mechanism of oxidation of both composite powders and monolithic ceramics of AlN–($TiB_2$–$TiSi_2$) system with different content of components were studied in the air up to 1450 °C under isothermal and non-isothermal conditions. It was established that the oxidation isotherms of monolithic ceramics follow the parabolic and paralinear rate law. According to the kinetic data and results of investigation of composition, morphology and structure of oxide films that are formed at different temperatures, the AlN–based ceramics containing up to 30% ($TiB_2$–$TiSi_2$) solid solutions are the corrosion-resistant and have the high adhesion of oxide layer in relation to substrate material. The activation energies of oxidation calculated for ceramics with 10% ($TiB_2$–$TiSi_2$) are: $E_1$ = 180 kJ/mol for the temperature range up to 1300 °C and $E_2$ = 630 kJ/mol at 1350–1450 °C. The change of activation energy value is associated with the change of oxide layer composition: at the oxidation till 1300 °C the oxides of individual elements are, mainly, formed on the samples while above 1350 °C the formation of very dense surface film containing β-tialite $Al_2TiO_5$ takes place.


*Keywords:* AlN; $Al_2O_3$; $Al_2TiO_5$; Composites; Oxidation

## 1. Introduction

There are literature data about high-temperature oxidation of both AlN[1–5] and $TiB_2$.[6–9] Concerning oxidation of pure AlN, it was established that the limiting stage defining the reaction mechanism was the oxygen diffusion through the scale. Hereby the amorphous aluminium oxide and $Al_{10}N_8O_2$ oxynitride are the oxidation products till 1100 °C while only α-$Al_2O_3$ above 1100 °C. The material on the base of pure AlN has a comparatively high corrosion resistance, but low magnitudes of mechanical characteristics. According to phase diagram of Ti–B–O system,[10] at the partial oxygen pressure near the atmospheric one and the high enough partial pressure of $B_2O_3$ ($10^{-9}$ Pa), the $TiO_2$ (rutile) is a stable reaction product. The lower titanium oxides are stable only at low pressures, and region of TiB existence is limited by narrow band between the fields of $TiB_2$ and lower titanium oxides stability. So, the main products of $TiB_2$ oxidation in air are $TiO_2$ and $B_2O_3$, the latter being intensively evaporated at elevated temperatures. However, the high-temperature corrosion of $TiB_2$[6–8] follows the parabolic oxidation law. It was shown that the additives being contained in the monolithic $TiB_2$ samples slow down the oxidation, forming the diffusion barriers at both matrix/scale and scale/gas interfaces as well as promoting the sintering of a scale. On the whole, pure $TiB_2$ has not a high oxidation resistance.

The oxidation of equimolar AlN–$TiB_2$ composite in the oxygen flow was studied[11] in the temperature range of 700–1300 °C. This material has high oxidation resistance at temperatures up to 1100 °C, but more intensive oxidation and formation of comparatively thick oxide layers restrict its application at higher temperatures. Nevertheless, the formation of aluminum borates ($Al_4B_2O_9$ and $Al_{18}B_4O_{33}$) by entrapment of boron oxide by alumina is very interesting because it reduces the evaporation of boron oxide in comparison with pure titanium boride.

* Corresponding author.
*E-mail address:* lavrenko@svitonline.com (V.A. Lavrenko).

0955-2219/02/$ - see front matter © 2002 Elsevier Science Ltd. All rights reserved.
PII: S0955-2219(02)00181-4

As for high-temperature oxidation of ($TiB_2$–$TiSi_2$) solid solution, there is only one paper[12] informing about the scale composition in the inner ($TiO_2$ anataz, $B_2O_3$) and outer ($TiO_2$ rutile, β-cristobalite, $B_2O_3$) scale layers in the temperature range of 1000–1200 °C. In particular, the oxidation of 20% $TiSi_2$ + 80% $TiB_2$ solid solution was studied. It was shown that during 7 h oxidation in air at 1200 °C the sample mass gain proved to be 6.2 mg/cm$^2$ whereas for pure $TiB_2$—29.5 mg/cm$^2$, i.e. the $TiSi_2$ additive increases the corrosion resistance of $TiB_2$. Besides, the $TiSi_2$ additive ensures the high plasticity of $TiB_2$-based ceramics at high temperatures.

## 2. Experimental

Kinetics of high-temperature oxidation in air up to 1450C of AlN–($TiB_2$–$TiSi_2$) composites as well as corresponding powder mixtures were studied under both isothermal and non-isothermal (at a heating rate of 15 °C/min) conditions by TG and DTA methods using a Setaram device. The composition and structure of interaction products were studied with the aid of XRD, EPMA, metallographic and SEM methods. XRD analysis was carried out in Cu$K_\alpha$ radiation using a DRON-3M device, determination of microstructure and elements distribution by EPMA using a Camebax 5X-50 device.

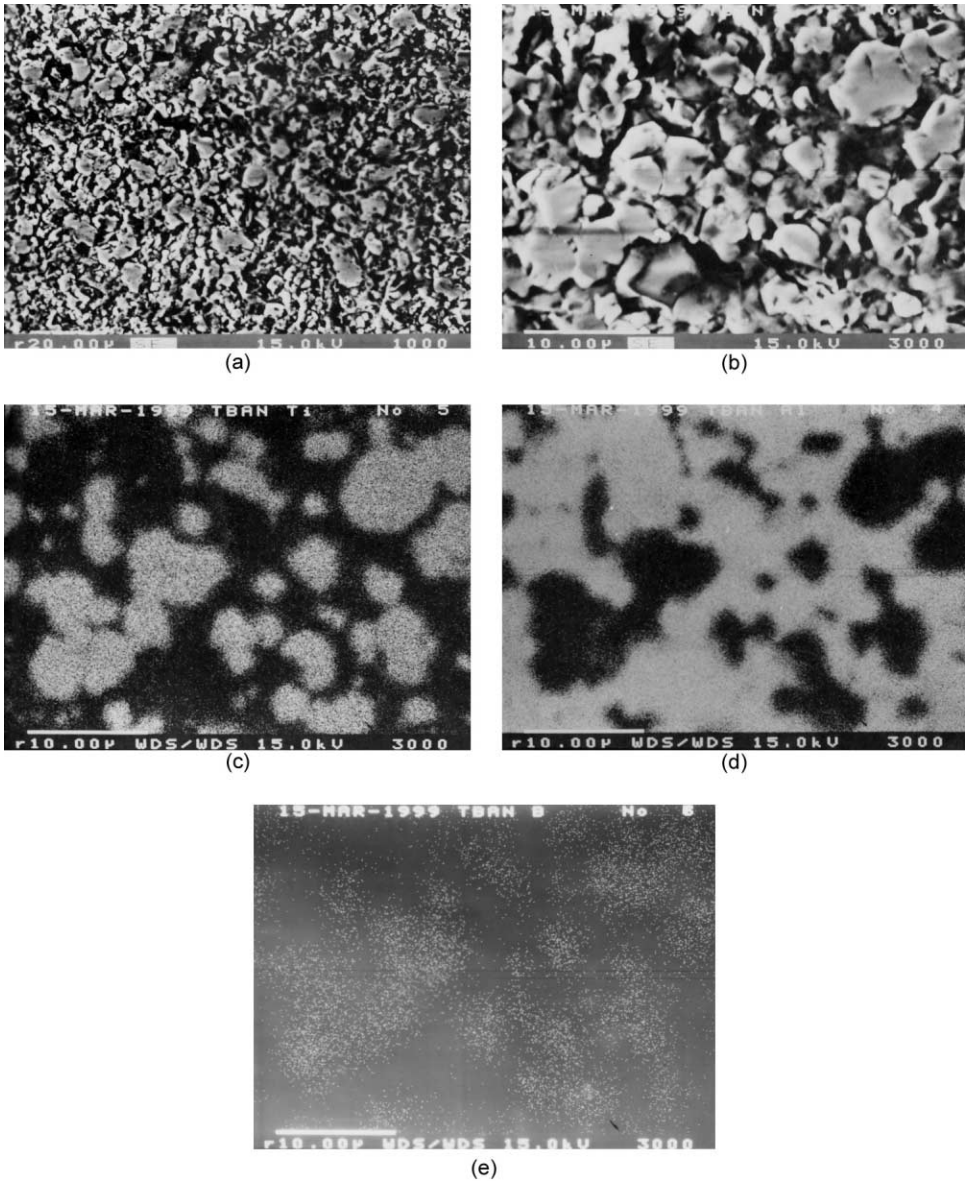


Fig. 1. Microstructure of 50% AlN–50% ($TiB_2$–$TiSi_2$) ceramics in secondary electrons [(a) × 1000, (b) × 3000] and in characteristic radiation [(c) Ti, (d) Al, (e) B, × 3000].

The monolithic ceramic samples were prepared using the sintering under pressure 30–40 MPa at 1760–1780 °C of AlN, $TiB_2$ and $TiSi_2$ powder mixtures crumbled in the planetary mill. The mixtures pointed out were ground in the drums lined with aluminium nitride. As grinding bodies the steel balls were used. The sample dimensions were 1.0 × 0.3 × 0.4 cm, the residual porosity of samples being <2%. The samples structure was homogeneous, fine-dispersion one, with the grain sizes <1–3 μm. One can see as an example the microstructure of 50% AlN–50% ($TiB_2$–$TiSi_2$) sample in secondary electrons (Fig. 1 a,b) and in characteristic radiation (Fig. 1c—Ti, d—Al, e—B). For all the ceramics compositions the initial sintered samples contained only crystalline phases (AlN, solid solution of $TiSi_2$ in $TiB_2$ with $TiSi_2$ concentration ~20 mass%, and Fe additive ~4–5%); the amorphous phases were not observed.

The samples with different AlN content (90, 70 and 50 mass% AlN) were investigated. In Tables 1 and 2, they are presented as 1, 2 and 3 samples, respectively. The powders under study were of the same composition, the particle size being <20 μm, initial weight of powder sample being 0.5 g.

## 3. Results and discussion

One can see in Fig. 2 the TG, DTA and DTG curves of non-isothermal oxidation of composite powders with 90 mass% AlN (a) and 50 mass% AlN (b). Oxidation of all studied powders of AlN–($TiB_2$–$TiSi_2$) system is a three-stage process characterized by three exothermal peaks on DTA-curves.

The temperature of first peak is the same (600–610 °C) for all compositions whereas the temperature of second peak is replaced from 1000 °C for 90% AlN to 900 °C (70% AlN) and 800 °C (powders with 50% AlN). The second peak is the most spread for 10 mass% ($TiB_2$–$TiSi_2$) content in the powder mixture; but the area under curve of this peak is minimum. As one can see in Fig. 2, a, the contribution of third (high-temperature) interaction stage in a summary heat evolution is the most one.

The endothermic region of DTA curves registered for the last (fourth) stage of non-isothermal heating of powders (for 90% AlN at $T > 1220$ °C and 50% AlN at $T > 950$ °C) is, probably, associated with an absorption of heat that is consumed for a sintering of a scale formed.

According to XRD data, the powders oxidized under non-isothermal heating up to 1300 °C contain β-$Al_2TiO_5$ (main phase), α-$Al_2O_3$, $TiO_2$ (rutile) as well as small amount of α-$SiO_2$ and $AlBO_3$ (traces). Hereby the aluminum titanate diffraction lines are somewhat modified on the account of dissolution of $Fe_2TiO_5$ in its lattice. The relative content of rutile and aluminum borate in the oxidized powders with 50% AlN proved to be significantly higher than that for 70% AlN and, especially, 90% AlN.

For monolithic ceramic samples the heat effects on DTA curves for all the oxidation stages are more feebly marked, the first peak being almost not pronounced. Herein the temperatures of second and third peaks are removed in the side of higher temperatures ~by 250 °C.

Table 1
Phase composition of scale on different AlN–($TiB_2$–$TiSi_2$)[a] ceramics (XRD data)

| Kind of samples | Temperature range °C | Composition of oxide film |
|---|---|---|
| 1 | 1200–1250 | $TiO_2$ (rutile), $Al_{10}N_8O_2$, α-$SiO_2$ (traces), $Fe_2O_3$ (traces) |
| | 1300–1350 | α-$Al_2O_3$, β-$Al_2TiO_5$, $Fe_2TiO_5$, $AlBO_3$ (small amount) |
| | 1400–1450 | α-$Al_2O_3$, β-$Al_2TiO_5$, (β-$Al_2TiO_5$- $Fe_2TiO_5$) solid solution,(α-$Al_2O_3$- $SiO_2$) solid solution |
| 2 | 1200–1250 | $TiO_2$ (rutile), $Al_{10}N_8O_2$, α-$SiO_2$ (traces), $Fe_2O_3$ (traces) |
| | 1300–1350 | α-$Al_2O_3$, β-$Al_2TiO_5$, $Fe_2TiO_5$, $AlBO_3$ (small amount) |
| | 1400–1450 | β-$Al_2TiO_5$, (β-$Al_2TiO_5$ – $Fe_2TiO_5$) solid solution, (α-$Al_2O_3$- $SiO_2$) solid solution, α-$Al_2O_3$ |
| 3 | 1200–1250 | $TiO_2$ (rutile), $Al_{10}N_8O_2$, α-$SiO_2$, $Fe_2O_3$ (traces) |
| | 1300–1350 | α-$Al_2O_3$, (β-$Al_2TiO_5$ – $Fe_2TiO_5$), (α-$Al_2O_3$- $TiO_2$), α-$SiO_2$, $AlBO_3$ |
| | 1400 | β-$Al_2TiO_5$, (β-$Al_2TiO_5$ – $Fe_2TiO_5$) solid solution, (α-$Al_2O_3$- $TiO_2$) solid solution, α-$SiO_2$ |

[a] $TiB_2$–20 mass% $TiSi_2$) solid solution.

Table 2
Constants $K_p$ (kg$^2$ m$^{-4}$ s$^{-1}$) of parabolic rate law for oxidation of the AlN–($TiB_2$ $TiSi_2$) ceramics

| Kind of composition | Temperature, °C | | | | | | | |
|---|---|---|---|---|---|---|---|---|
| | 1200 | 1220 | 1250 | 1275 | 1300 | 1350 | 1400 | 1450 |
| 1 | $1.51\times10^{-9}$ | | $2.26\times10^{-9}$ | | $3.82\times10^{-9}$ | $1.06\times10^{-8}$ | $4.67\times10^{-8}$ | $1.65\times10^{-7}$ |
| 2 | $1.33\times10^{-8}$ | $1.8\times10^{-8}$ | | $7.8\times10^{-8}$ | $1.03\times10^{-7}$ | $2.95\times10^{-7a}$ | $3.25\times10^{-7a}$ | |
| 3 | $7.92\times10^{-8a}$ | | $2.58\times10^{-7a}$ | | | | | |

[a] Quasi-parabolic oxidation (with some throwing about of points).

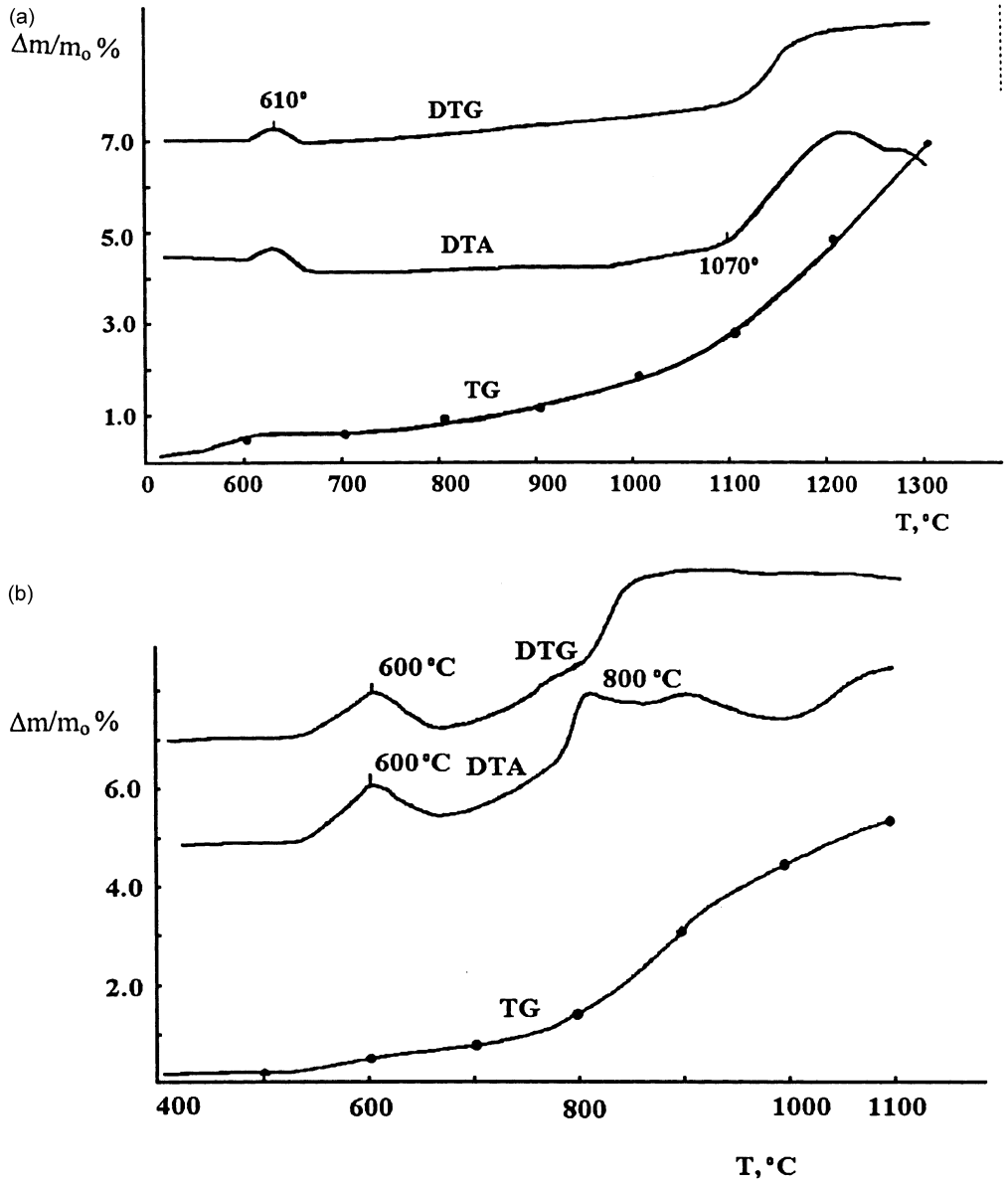


Fig. 2. High-temperature oxidation of 90% AlN–10% ($TiB_2$–$TiSi_2$) (a) and 50% AlN–50% ($TiB_2$–$TiSi_2$) (b) composite powders.

The length of third peak field is different for different ceramics (in the range of 1350–1450 °C).

According to XRD and EPMA data, the first, most weak DTA peak is, obviously, connected with a heat effect of reaction

$$TiB_2 + O_2 \rightarrow TiO_2 \text{ rutile} + B_2O_3 \quad (1)$$

At the second stage the formation of silicon dioxide and aluminum oxynitride takes place

$$TiSi_2 + O_2 \rightarrow TiO_2 \text{ (rutile)} + SiO_2 (\alpha\text{-quartz}) \quad (2)$$

$$AlN + O_2 \rightarrow Al_{10}N_8O_2 + N_2 \quad (3)$$

along with the oxidation of Fe additive being contained in a drum charge on the account of a grinding

$$Fe + O_2 \rightarrow Fe_2O_3 \quad (4)$$

For the third stage the total exothermal effect is defined by a proceeding of four reactions:

$$Al_{10}N_8O_2 + O_2 \rightarrow \alpha\text{-}Al_2O_3 + N_2 \quad (5)$$

$$Al_2O_3 + TiO_2 \rightarrow \beta\text{-}Al_2TiO_5 \text{ (a tialite structure)} \quad (6)$$

$$Fe_2O_3 + TiO_2 \rightarrow Fe_2TiO_5 \text{ (a bruskite-like lattice)} \quad (7)$$

$$Al_2O_3 + B_2O_3 \text{ melt} = AlBO_3 \quad (8)$$

The reaction (6) gives the most contribution to the total heat evolution.

So, the boron oxide, formed in the first oxidation period, is melted and in the further partially interacts with $\alpha$-$Al_2O_3$ (another part of $B_2O_3$ is evaporated). Hereby $AlBO_3$ is formed, its traces, sometimes small amounts, being found by XRD method (see Table 1). It must be noted that at the temperatures more than 1400 °C aluminum borate was not found in the scale, obviously, due to its decomposition and $B_2O_3$ rapid evaporation. Because of a prevailing exothermal effect of ($TiB_2$–$TiSi_2$) oxidation itself and comparatively small amounts of $B_2O_3$, the endothermic sections on DTA-curves, associated with $B_2O_3$ melting and evaporation, were not observed in our tests. However, in the cases of larger ($TiB_2$–$TiSi_2$) content in the ceramics studied, the less dense oxidation layers were formed, mainly, resulting from more essential contribution of melted $B_2O_3$ evaporation. Because composition and condition of the protective oxidation surface layer

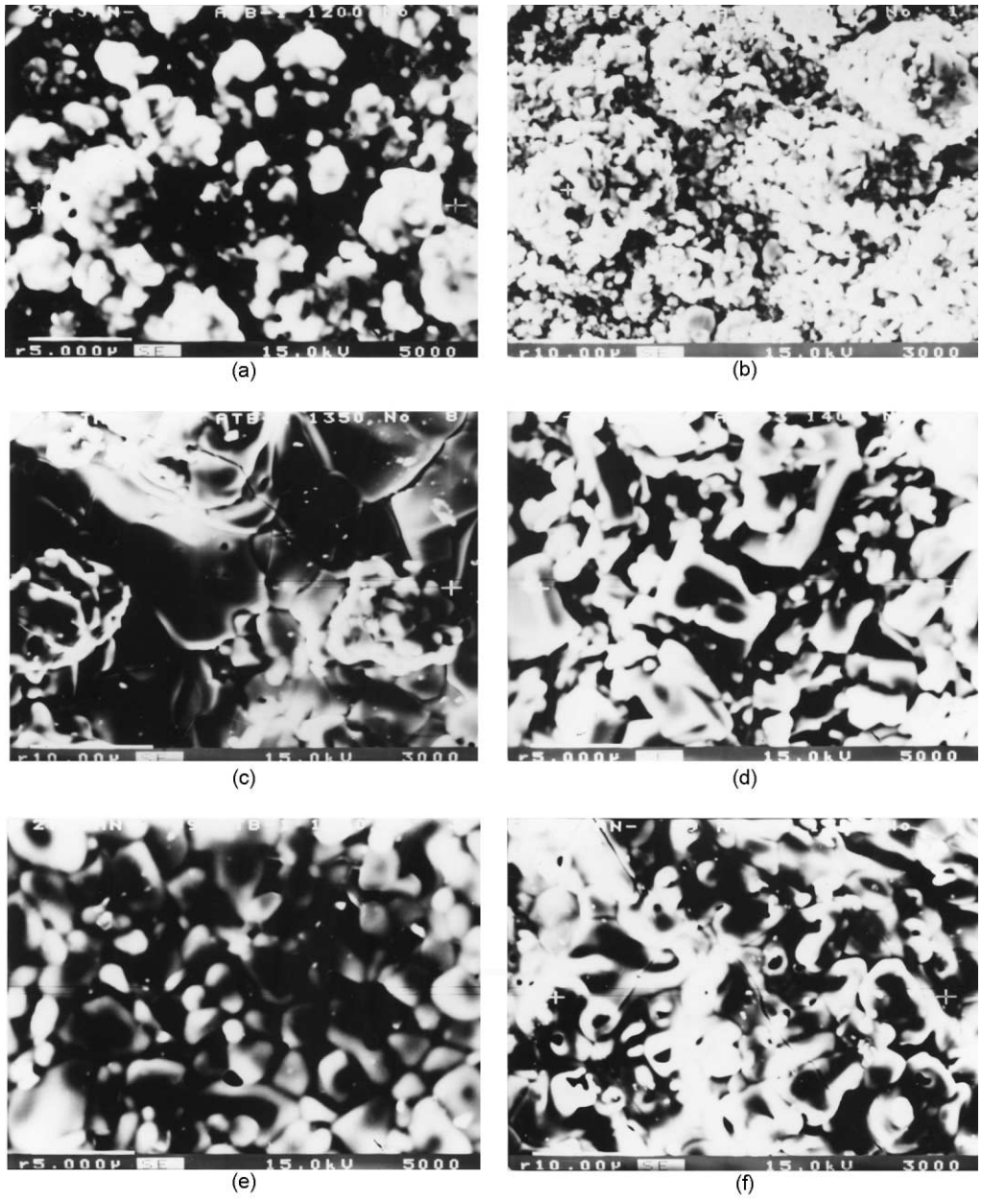


Fig. 3. Structure of oxide film formed on AlN–($TiB_2$–$TiSi_2$) ceramics at different temperatures: (a) 90% AlN–10% ($TiB_2$–$TiSi_2$), 1200 °C, × 5000; (b) 70% AlN–30% ($TiB_2$–$TiSi_2$), 1200 °C, × 3000; (c) 70% AlN–30% ($TiB_2$–$TiSi_2$), 1350 °C, × 3000; (d) 50% AlN–50% ($TiB_2$–$TiSi_2$), 1400 °C, × 5000; (e) 90% AlN–10% ($TiB_2$–$TiSi_2$), 1450 °C, × 5000; (f) 70% AlN–30% ($TiB_2$–$TiSi_2$), 1500 °C, × 3000.

determine the oxygen diffusion into the materials, it can be one of the main factors in the oxidation behavior of ceramic materials containing borides.

With the aid of XRD, EPMA, SEM and metallographic analyses, it was established that the oxide film formed at the oxidation of ceramics with 90% AlN at 1200 °C (Fig. 3a) consisted of a light phase as large oval globules (conglomerations of smaller grains, ~2.5–3.0 μm) as well as more dark loose "matrix" phases with the grain sizes of 3.5–3.9 μm. The globules pointed out contain titanium, oxygen and iron (Fig. 4a,b). The identified phases are $TiO_2$ (rutile), aluminum oxynitride, as well as small amounts of α-$SiO_2$ and $Fe_2O_3$ (see also Table 1).

At 1300 °C the crystallites of matrix phases of oxide film are small enough, they have a plate-like shape with the ground cut grains, sometimes as column-like grains. This film proved to be tightly sintered, it is characterized by high adhesion as to a substrate. It consists of three main phases: β-$Al_2TiO_5$ (an average grain size ~1.5–1.7 μm), $Fe_2TiO_5$, and α-$Al_2O_3$ alloyed with α-$SiO_2$ (an average grain size ~1.7 μm). The corresponding elements distribution is presented in Fig. 4c,d). In this film a small amount of $AlBO_3$ phase is found by XRD method as well.

At 1450 °C a very dense ultra-dispersion film forms on the samples containing 90% AlN (Fig. 3e). This film

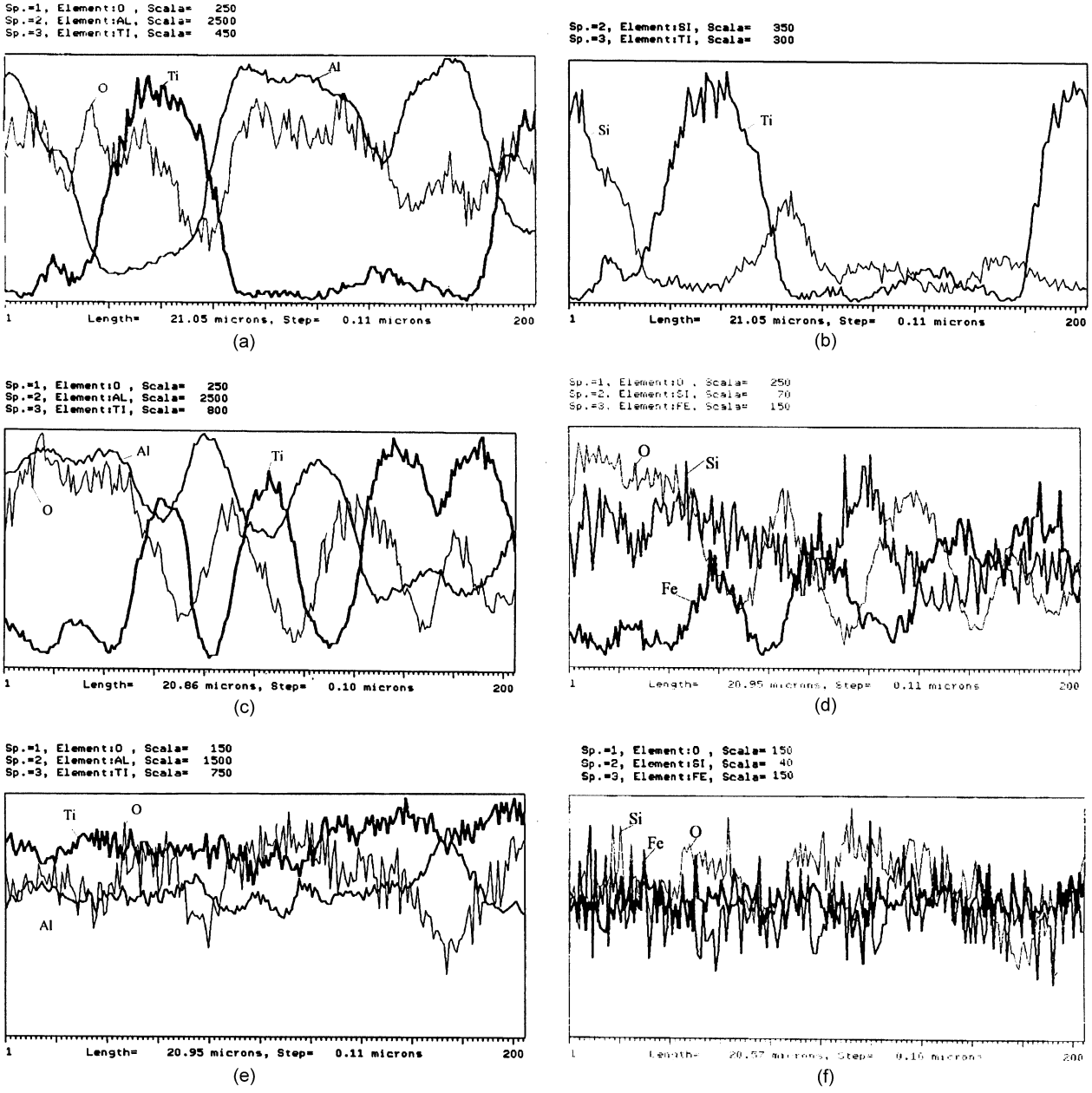


Fig. 4. Distribution of elements in oxide film on 90% AlN–10% ($TiB_2$–$TiSi_2$) sample at different oxidation temperatures: (a, b) 1200 °C; (c, d) 1300 °C; (e, f) 1450 °C.

has an average grain size $<0.5$ μm (only sometimes there are the solitary grains $\sim 0.8$ μm).

It is characterized by an uniform distribution of elements—Al, Ti, Fe, Si, O (Fig. 4e,f) and can testify to a formation of β-$Al_2TiO_5$, solid solution of $Fe_2TiO_5$ in β-$Al_2TiO_5$ as well as a presence of α-$Al_2O_3$ with $SiO_2$ dissolved in its lattice. The essential crushing up of crystallites can be associated with the eutectic system formation.[13] Apparently, the sintering of oxide layer is caused by a presence of a liquid phase.

According to XRD (Table 1) and EPMA study of oxide film formed on monolithic 70% AlN–30% ($TiB_2$–$TiSi_2$) ceramics at 1200 °C (Figs. 3b and 5a,b), it consists of $Al_{10}N_8O_2$, $TiO_2$ (rutile) alloyed with $Fe_2O_3$, and α-quartz with the rutile inclusions (a particle size $\sim 1.2$–1.5 μm). There are also the globules of 3.5–4.8 μm, the latter growing together with the smaller grains.

At 1300 °C the oxide film on 70% AlN–30% ($TiB_2$–$TiSi_2$) samples is also a fine-grain one. It consists of β-$Al_2TiO_5$, $Fe_2TiO_5$, $AlBO_3$ (small amount), α-$Al_2O_3$,

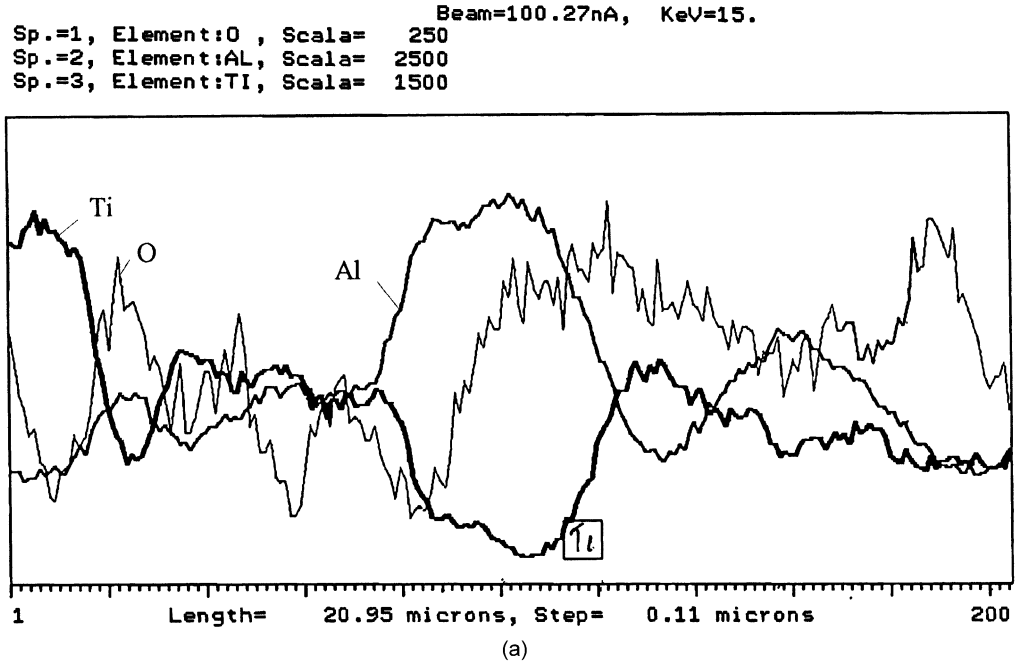


(a)

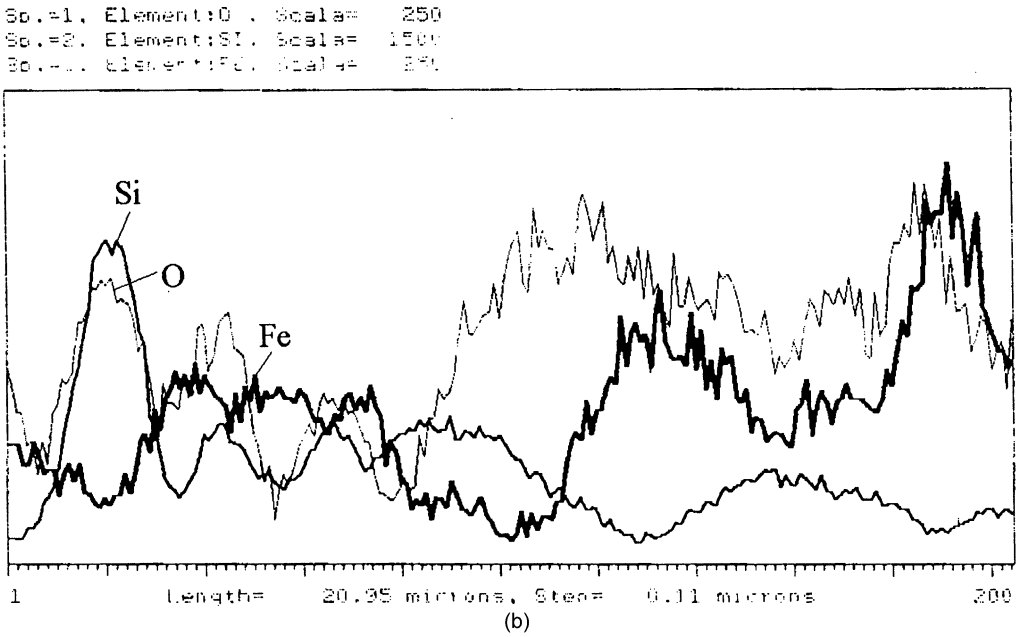


(b)

Fig. 5. Distribution of elements in oxide film on 70% AlN–30% ($TiB_2$–$TiSi_2$) sample at different oxidation temperatures: (a, b) 1200 °C; (c, d) 1350 °C.

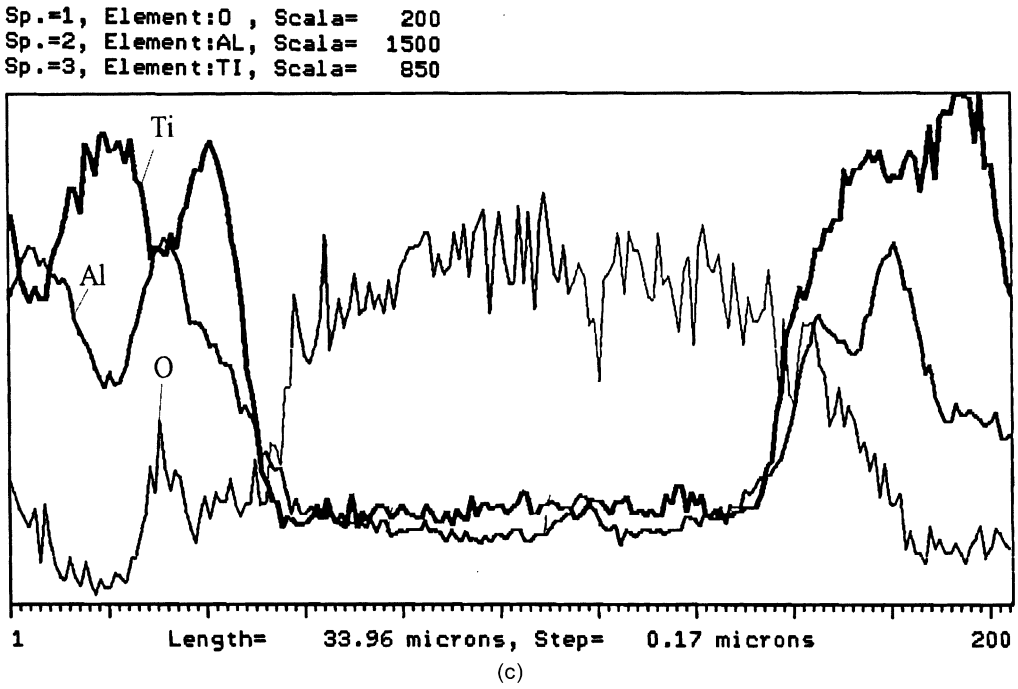


(c)

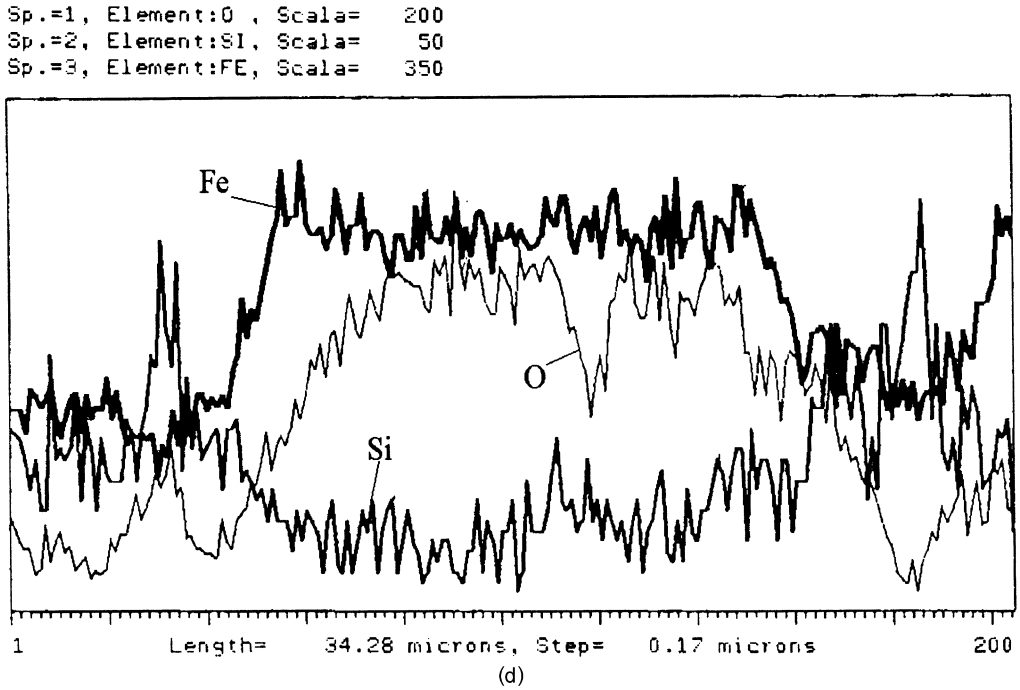


(d)

Fig. 5. (*continued*)

and $SiO_2$, the grain sizes of last two phases being ~1.7–2.1 μm. At 1350 °C a significant growth of β-tialite grains is observed. As a result of their recrystallisation the $Al_2TiO_5$ plates form (Fig. 3c), and a number of $Fe_2TiO_5$ globules essentially decreases, they disintegrate to the smaller grains (the elements distribution see in Fig. 5c,d).

At 1450 °C the β-$Al_2TiO_5$ and solid solution of $Fe_2TiO_5$ in β-$Al_2TiO_5$ are the main phases of the film on 70% AlN–30% ($TiB_2$–$TiSi_2$) ceramics (Table 1, Fig. 3f) however, there are also the separate grains of solid solution of $SiO_2$ in α-$Al_2O_3$. Hereby some large grains of silicon dioxide (~5–6 μm) are discretely placed near the film/substrate boundary while the separate rutile grains are discretely arranged near the film/gas interface.

The oxide film formed at the oxidation of 50% AlN–50% ($TiB_2$–$TiSi_2$) ceramics samples at 1200 °C is characterized by a fine-dispersion structure with the maximum value of grains <2 μm . It contains $Al_{10}N_8O_2$,

$Fe_2O_3$ (the iron diffuses to a surface), $TiO_2$, solid solution of $Fe_2O_3$ in $TiO_2$, and also some amount of $\alpha$-$SiO_2$, according to Fig. 6 a,b.

At 1400 °C the scale on these ceramics contains the ($Al_2O_3$–$TiO_2$) solid solution with a grain size $<3$ μm, fine-dispersion phases of $\beta$-$Al_2TiO_5$ and solid solution of $Fe_2TiO_5$ in $Al_2TiO_5$ with an average grain size $<1.5$ μm, and also the solitary grains of $\alpha$-$SiO_2$ (Figs. 3d and 6c,d).

Thus, with increasing content of $TiB_2$–$TiSi_2$ a shift of the oxidation processes to lower temperatures was observed. On the base of TG and DTA data of non-isothermal oxidation as well as isotherms of the dependence of samples mass gain on the exposure time, one can conclude that the ceramics of 90% AlN–10% ($TiB_2$–$TiSi_2$) system proved to be the most oxidation-resistant (Fig. 7). The mass gain per a unit of a surface area resulting from the samples heating in air at 1350 °C during 120 min for the 90% AlN–10% ($TiB_2$–$TiSi_2$) material is 0.7, 70% AlN–30% ($TiB_2$–$TiSi_2$)—4.5, and 50% AlN–50% ($TiB_2$–$TiSi_2$)–6.0 mg/cm$^2$ (Fig. 8).

It has been established that for the first out of these ceramics the oxide films obtained are the dense enough, practically without pores, uniform, with a sharp border

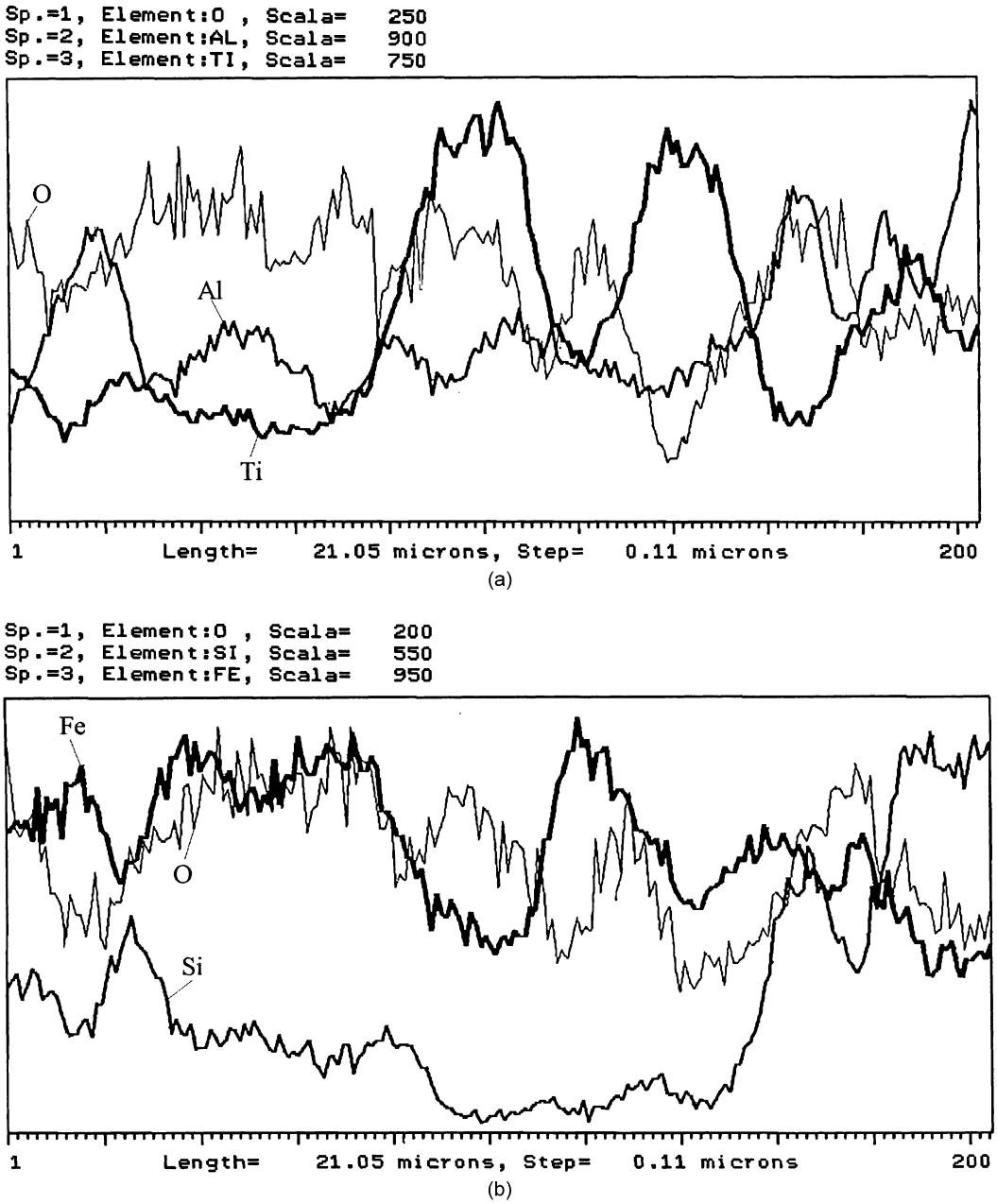


Fig. 6. Distribution of elements in oxide film on 50% AlN–50% ($TiB_2$–$TiSi_2$) sample at different oxidation temperatures: (a, b) 1200 °C; (c, d) 1400 °C.

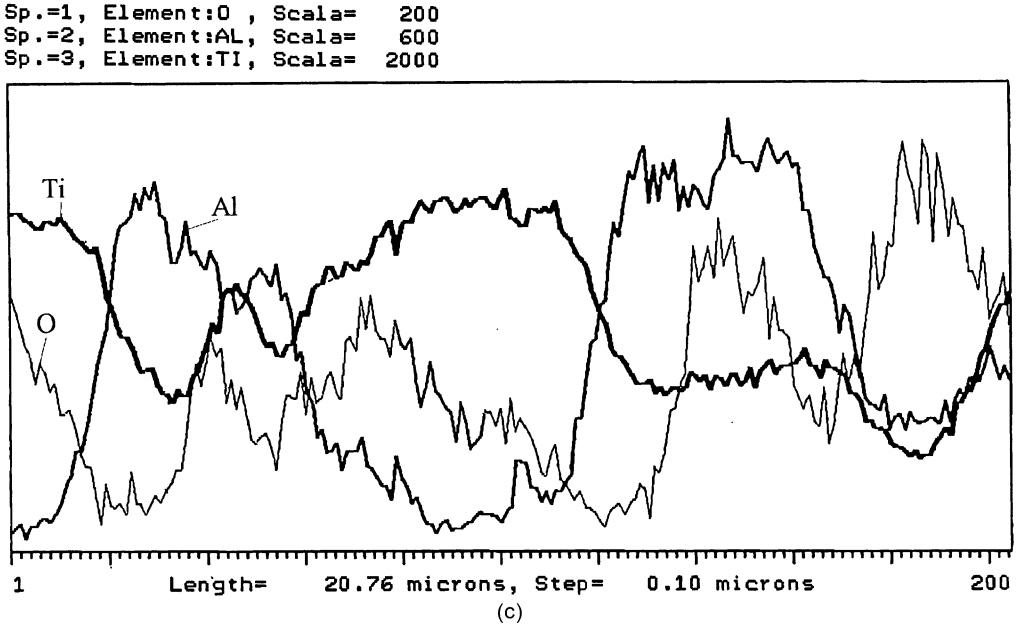


(c)

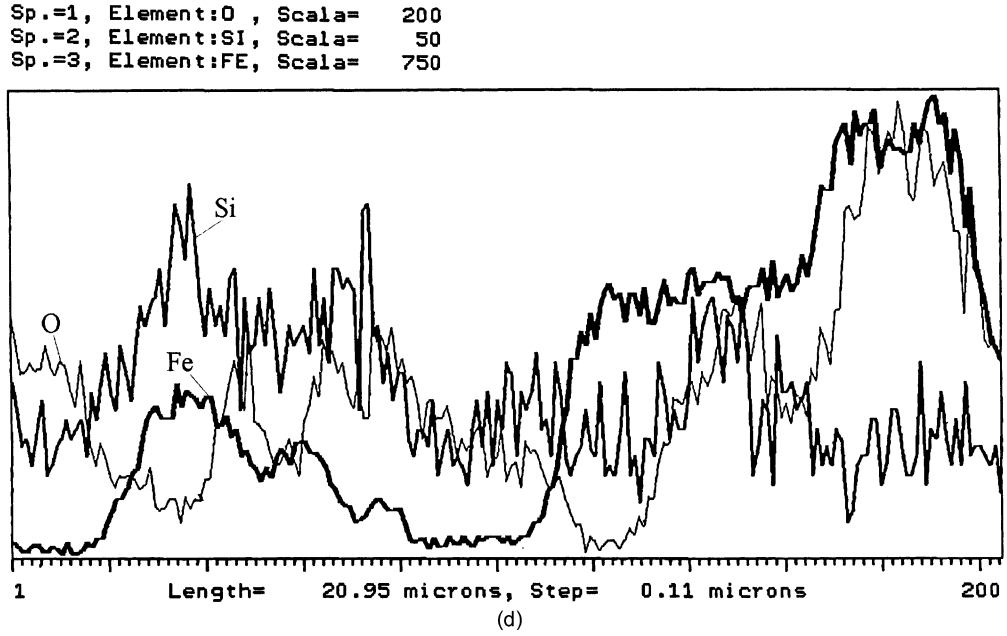


(d)

Fig. 6. (*continued*)

between substrate and scale. However, in the case of ceramics with 50% ($TiB_2$–$TiSi_2$), the scale formed at 1300–1400 °C proved to be more friable—on the account of larger amount of aluminum borate and its further decomposition with $B_2O_3$ evaporation. Namely in this case the oxygen diffusion into the material is significantly accelerated, and oxidation process occurs in the bulk of material too. The final thickness of oxide layer on different ceramics is differed, depending on the ($TiB_2$–$TiSi_2$) content, and is equal to 14...25 μm.

For initial stages of oxidation, almost in all the cases, the isothermal curves of mass gain follow the parabolic law of the dependence of oxidation rate on time (τ). Taking into account the experimental oxidation isotherms (for the ceramics with 90% AlN see Fig. 7), on the base of $(\Delta m/S)^{2=}f(\tau)$ linear dependence (Fig. 9) obtained, the constants of parabolic rate law were calculated. They are presented in Table 2 for different ceramics composition. It must be noted that vaporization of $B_2O_3$, especially in the case of 50% AlN – 50% ($TiB_2$ – $TiSi_2$) ceramics, can exert a strong influence upon the deviation of kinetic curves observed from a parabolic dependence. Above 1250 °C the oxidation of these ceramics always obeys paralinear or linear law.

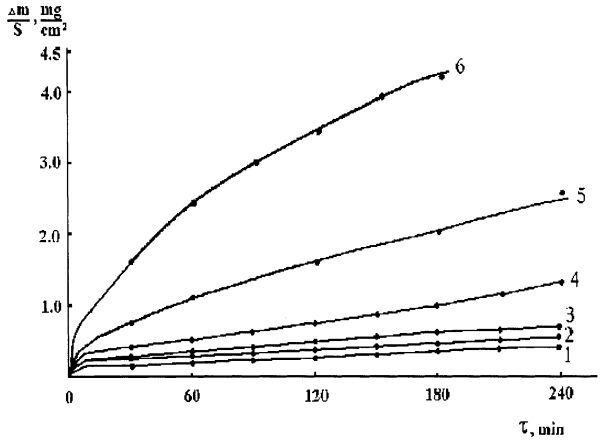


Fig. 7. Oxidation isotherms for 90% AlN–10% ($TiB_2$–$TiSi_2$) ceramics at temperatures (°C): (1) 1200, (2) 1250, (3) 1300, (4) 1350, (5) 1400, (6) 1450.

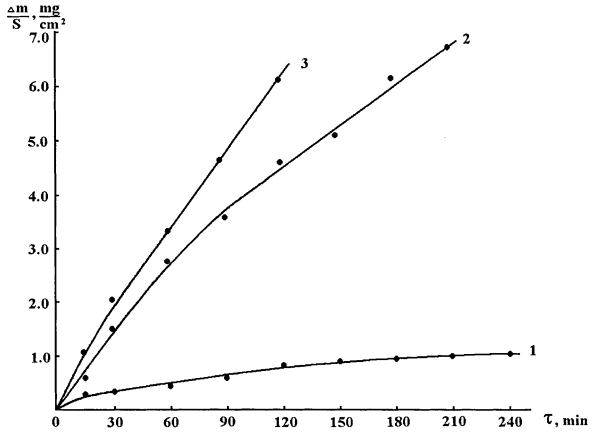


Fig. 8. Oxidation isotherms at 1350 °C for ceramics: (1) 90% AlN–10% ($TiB_2$–$TiSi_2$), (2) 70% AlN–30% ($TiB_2$–$TiSi_2$), (3) 50% AlN–50% ($TiB_2$–$TiSi_2$).

One can see in Table 2 a significant rise of oxidation rate at an increase of ($TiB_2$–$TiSi_2$) content in the ceramics samples.

According to Arrhenius plot, on the base of dependence of logarithm of oxidation rate constants on reciprocal temperature, the values of apparent activation energy were calculated [see Fig. 10 for the material with 10% ($TiB_2$–$TiSi_2$)]. So, for these ceramics $E_1 = 180$ kJ/mol in the temperature range of 1200–1300 °C and $E_2 = 630$ kJ/mol in the interval of 1350–1450 °C while for 70% AlN–30% ($TiB_2$–$TiSi_2$) ones in the range of 1200–1350 °C the oxidation is characterized by only value of $E = 400$ kJ/mol.

The change of activation energy for 90% AlN–10% ($TiB_2$–$TiSi_2$) ceramics is associated with a change of oxidation mechanism in the temperature range of ~1300–1350 °C. In this case, up to 1300 °C the oxidation is limited by oxygen diffusion into a depth of sample as well as an opposite diffusion of material components through a film containing individual oxides

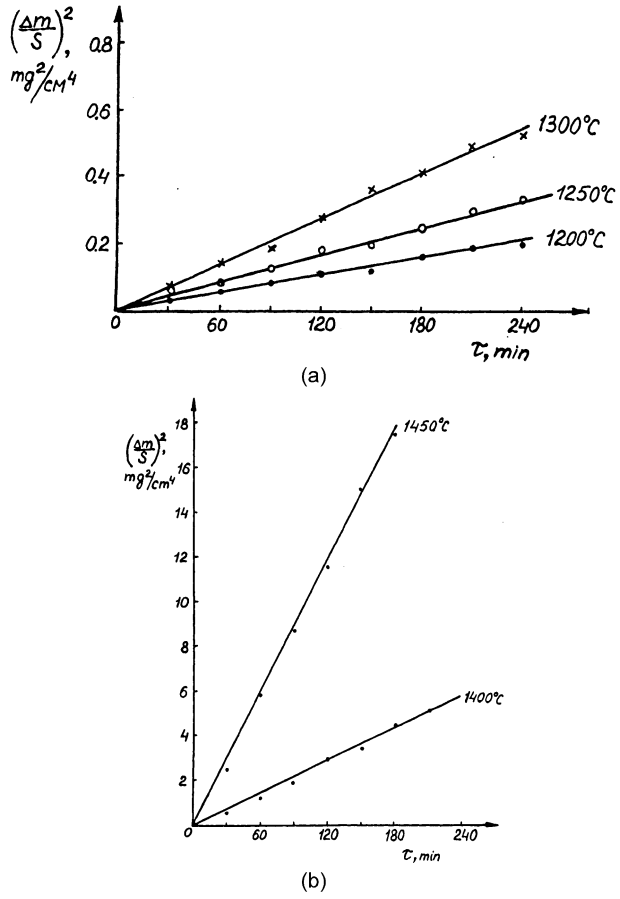


Fig. 9. Plots for calculation of constants of parabolic rate law for 90% A1N–10% ($TiB_2$–$TiSi_2$) ceramics at oxidation temperatures: (a) 1200, 1250 and 1300 °C; (b) 1400 and 1450 °C.

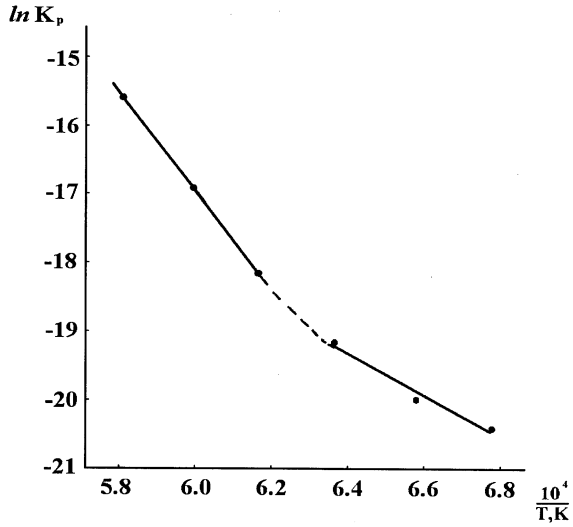


Fig. 10. Dependence of the rate constant of parabolic oxidation law on the reciprocal temperature for 90% AlN–10% ($TiB_2$–$TiSi_2$) ceramics.

of elements. At the temperatures above 1350 °C, the oxidation is already limited by oxygen diffusion through a formed exceptionally dense surface film of β-$Al_2TiO_5$

and solid solution of $Fe_2TiO_5$ in β-$Al_2TiO_5$ that leads to a slowing down of the process rate because of a sharp rise of activation energy.

In the case of interaction of 70% AlN–30% ($TiB_2$–$TiSi_2$) material with oxygen, the β-tialite formation is already observed in oxide film at ~1250 °C, the oxidation of these ceramics being defined by only value of the apparent activation energy.

In order to increase the corrosion resistance of AlN–($TiB_2$–$TiSi_2$) ceramics, the preliminary oxidation at lower temperature is used. In such cases the protective oxide layers are formed a priori to prevent from the further oxidation. The sample of 70% AlN–30% ($TiB_2$–$TiSi_2$) ceramics preliminarily oxidized at 1120 °C during 3.5 h (Fig. 11, curve 1) then was oxidized at 1350 °C (curve 3); the parabolic rate constant $K_p = 2.95.10^{-7}$ kg$^2$ m$^{-4}$ s$^{-1}$. After such treatment the same sample was oxidized at 1400 °C during 3.5 h. Hereby the mass gain (curve 2) proved to be significantly less, the $K_p = 5.5.10^{-8}$ kg$^2$ m$^{-4}$ s$^{-1}$ being by 5.4 times less than that for 1350 °C. Of course, in these cases, the calculation of parabolic rate constants has a conditional character because of a deviation of kinetic curves obtained from parabolic dependence, resulting from the boron oxide volatilization.

Thus, on the base of kinetic data (Table 2) and data concerning composition, morphology and structure of oxide films, among the materials studied the AlN–based ceramics with 10% ($TiB_2$–$TiSi_2$) proved to be the most corrosion-resistant, with a high adhesion of oxide layer as to a substrate material.

The features of oxide film formation on these materials depend on many factors. First of all, one can take into account the composition of ceramics, rates of oxidation of different components and intermediate products

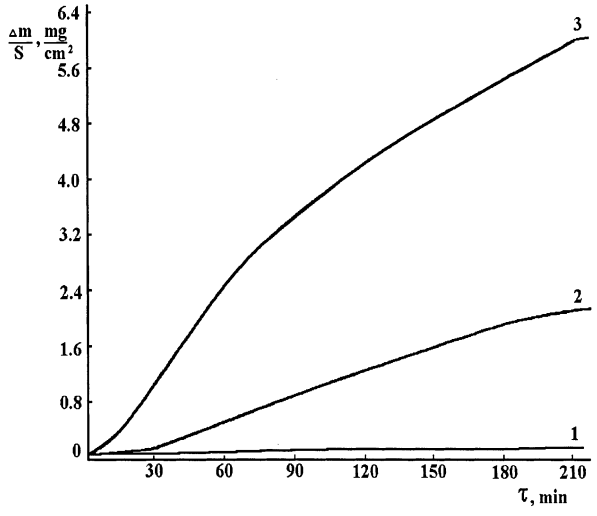


Fig. 11. The effect of preliminarily oxidation of 70% AlN–30% ($TiB_2$–$TiSi_2$) ceramics on a rise of their corrosion resistance. The sequence of sample heating: 1120 °C (curve 1); 1350 °C (curve 3); 1400 °C (curve 2).

according to (1), (2), (3), (4) and (5) reactions. The kinetics of both solid-phase (6), (7) reactions and solid-liquid (8) reaction, mechanism of diffusion of oxygen and solid components as well as boron oxide melting and evaporation also exert the significant effect on the ceramics oxidation behavior. Besides, one has to take into account a mutual solubility of titanate and oxide phases and also a possibility of eutectics formation in the appropriate thermodynamic systems.

In the case of 90% AlN–10% ($TiB_2$–$TiSi_2$) and 70% AlN–30% ($TiB_2$–$TiSi_2$) materials, under the definite conditions of high-temperature oxidation, the formation of a gradient structure, in fact, takes place. Hereby a dense growing together of a surface material layer with a base occurs due to a very high adhesion. The mechanical properties of such gradient materials at high temperatures in air may be significantly better than those of the ceramics without protective surface layers.

## 4. Conclusion

1. The composition and structure of AlN–($TiB_2$–$TiSi_2$) ceramics containing ~5% Fe additive as well as oxidation conditions exert a strong influence upon the kinetics and mechanism of scale formation. At short times of exposure in air and comparatively low temperatures (1200–1300 °C), $TiO_2$ rutile, boron oxide, aluminum oxynitride, and α-quartz are formed. At longer oxidation and higher temperatures (1350–1450 °C) β-$Al_2TiO_5$ (tialite) and a solid solution of $Fe_2TiO_5$ in β-$Al_2TiO_5$ are the main interaction products. Herein the small amounts of solid solutions of $TiO_2$ and $SiO_2$ in α-$Al_2O_3$ are present as well.
2. The values of apparent activation energy of oxidation of 90% AlN–10% ($TiB_2$–$TiSi_2$) ceramics calculated on the base of experimental kinetic data according to the Arrhenius equation are: $E_1 = 180$ kJ/mol for the temperature range of 1200–1300 °C and $E_2 = 630$ kJ/mol for the interval of 1350–1450 °C.
3. The AlN–($TiB_2$–$TiSi_2$) ceramics studied, especially with 10% ($TiB_2$–$TiSi_2$) solid solution content, have a high oxidation resistance in air up to 1450 °C, mainly, on the account of aluminum titanate formation in the outer scale layer.
4. In the case of these ceramics high-temperature oxidation, the formation of fine-dispersion structure takes place. Hereby a growing together of surface layer with a base occurs due to a very high adhesion, the gradient materials with protective outer layer forming.

## Acknowledgements

This study was supported by European Commission under INTAS grant 96–2232.

## References

1. Lavrenko, V. A. and Alexeev, A. F., Oxidation of sintered aluminium nitride. *Ceram. Intern*, 1983, **9**(3), 80–82.
2. Bellosi, A., Landi, E. and Tampieri, A., Oxidation behavior of aluminium nitride. *J. Mater. Res*., 1997, **8**(3), 566–572.
3. Katnani, A. D. and Papathomas, K. I., Kinetics and initial stages of oxidation of aluminium nitride: thermogravimetric analysis and X-ray photo-electron spectroscopy study. *J. Vac. Sci. Techn*., 1987, **A5**(4), 1335–1339.
4. Suryanarayana, D., Oxidation kinetics of aluminium nitride. *J. Am. Cer. Soc*., 1990, **73**(4), 1108–1110.
5. Gogotsi, Yu.G. and Lavrenko, V. A., *Corrosion of High-performance Ceramics*. Springer, Berlin, 1992.
6. Lebugle, A. and Montel, G., High-temperature oxidation of titanium diboride. *Rev. Int. Hautes. Temp*, 1974, **11**, 231–234.
7. Voitovich, R. F. and Pugach, E. A., High-temperature oxidation of $TiB_2$. *Powder Metallurgy*, 1975, **2**, 57–61 (in Russian).
8. Cuortois, C., Desmaison, J. and Tawil, H., Oxidation behaviour of $TiB_2$. *J. Phys. IV*, 1993, **C9**(N3), 843–853.
9. Voitovich, V. B., Lavrenko, V. A. and Adejev, V. M., High-temperature oxidation of titanium diboride of different purity. *Oxid. Metals*, 1994, **42**(1/2), 145–161.
10. Katz, J. D., Blake, R. D. and Scherer, C. P., Phase-stability diagram of Ti-B-O system. *Ceram. Eng. Sci. Proc*, 1989, **10**, 854–859.
11. Schneider, S. V., Desmaison-Brut, M., Gogotsi, Yu.G. and Desmaison, J., Oxidation behavior of a hot isostatically pressed $TiB_2$-AlN composite. *Key Eng. Mater*., 1996, **113**, 49–58.
12. Pugach, E. A., Golovko, E. I. and Dvorina, L. I., High-temperature oxidation of $TiB_2$ –$TiSi_2$ alloys. *Powder Metallurgy*, 1977, **2**, 34–37 (in Russian).
13. Berezhnoy, A. S., *Multi-component Oxide Systems*. Naukova dumka, Kiev, 1970 (in Russian).